Biophysical Journal, Volume *119*

Supplemental Information

Constitutive Model of Erythrocyte Membranes with Distributions of Spectrin Orientations and Lengths

Zhe Feng, Richard E. Waugh, and Zhangli Peng

APPENDIX A. Numerical solution of pipette aspiration using an ODE model

The deformation of the aspirated cell is assumed to be radially symmetric. An initial resting state is defined as a biconcave disc according to the formulations of Fung (1)

$$z(r) = (c_0 + c_1 {r_0}^2 + c_2 {r_0}^4)\sqrt{1 - (r_0/R_0)^2} \tag{S1}$$

where z is the half thickness of the cell, r_0 is the radial coordinate, and R_0 is the cell radius. (Note, the subscript "0" indicates that this is the radial position of a material element in the undeformed shape.) This expression is integrated to obtain the distance along the surface, $s_0(r_0)$, and the area of the surface inside the coordinate value $A_0(r_0)$. This information is saved in a look-up table for determination of r_0 for a given A_0. (Note that once the integration passes the edge of the undeformed cell, the relevant area is the area of one half of the cell plus the area outside the coordinate value r_0.)

To solve for the distribution of stress and density on the deformed surface we integrate the tangential force balance as

$$\frac{\partial \tau_1^{sk}}{\partial s} = -\frac{1}{r}\left(\tau_1^{sk} - \tau_2^{sk}\right)\cos(\theta) \tag{S2}$$

where s is the distance along the surface of the deformed shape, r is the radial coordinate of the deformed shape τ_1^{sk} and τ_2^{sk} are the meridional and the circumferential principal force resultants, and θ is the angle between the surface normal and the axis of symmetry ($\cos\theta = dr/ds$). The integration must be completed under the constraint that the mass of membrane skeleton is constant

$$\oint \rho dA = \oint \rho\, 2\pi r ds = \oint \rho_0 dA_0 \tag{S3}$$

Note that the resting density ρ_0 is assumed to be constant and that $\rho/\rho_0 = 1/(\lambda_1\lambda_2)$. The constraint can be written as

$$\oint \frac{\rho}{\rho_0}\, 2\pi r ds = A_0 \tag{S4}$$

This relationship is also the basis for determining r_0, the radial position of the instantaneous material element in the undeformed state. This is needed to calculate $\lambda_2 = r/r_0$. Therefore, we use the fact that

$$\frac{\mathrm{d}A_0}{\mathrm{d}s} = \frac{2\pi r}{\lambda_1 \lambda_2} \tag{S5}$$

and use the look-up table constructed from the unstressed geometry to find $r_0(A_0)$. The integration of the tangential force balance proceeds with s as the independent variable. The shape of the surface is assumed to be known: a hemispherical cap radius R_p, a section of cylinder with radius R_p and length L_p - R_p, and a biconcave shape described by Eq. S1 with the maximum radius calculated to maintain the total area of the shape a constant

$$2\pi {R_p}^2 + 2\pi R_p\left(L_p - R_p\right) + A_{disk} = A_0 \tag{S6}$$

Because the shape is fixed, for any s, the radius r and the angle to the surface normal θ are known. It is fairly straightforward to integrate the three simultaneous first order differential equations for the dependent variables A_0 and τ_1.

Starting the integration at the tip of the pipette, a guess is made for the starting value of $\lambda_o = \lambda_1 = \lambda_2$ at the tip. One approach is to use this starting value to integrate over the entire cell surface and adjust the value of λ_o in repeated tries until the mass conservation condition is met. This approach is problematic because of singularities that occur when λ_o is too small and the integrated value of A_0 is smaller than the cell area. In this case r_o goes to zero, and λ_2 becomes infinite. A more robust approach is to choose a location (for example the base of the projection at the edge of the pipette), and calculate two sets of solution values for A_0 and τ_1 at the chosen location, one starting from the tip of the projection for a range of starting values for λ_o, and one starting at the

opposite pole at the center of the disk for a range of starting values λ_d. If we let the integrated A_0 on the disk be A_{0d}, and the integrated A_0 of the projection be A_{0p}, then we require that

$$A_0 - A_{0d} = A_{0p} \tag{S7}$$

We can then plot two curves, one of (A_0 - A_{0d}) as a function of τ_1^{sk} (or equivalently, λ_1) at $r = R_p$ determined from the disk integration, and one of A_{0p} as a function of τ_1^{sk} (or equivalently, λ_1) at the base of the projection from the integration over the projection. The solution occurs where these two curves cross. The corresponding values for λ_o and λ_d are the starting values for the solution satisfying continuity of stress and mass conservation over the cell surface. Curves showing the solution intersections for a series of projection lengths is shown in Figure S1, and the distribution of density and shear force resultant are shown in Figures S2 and S3. The distribution of the principal stretch ratios is shown in Figure S4. The reader is advised that this method is not efficient, and may require significant computing time, particularly for cases where the values of initial molecular lengths are distributed.

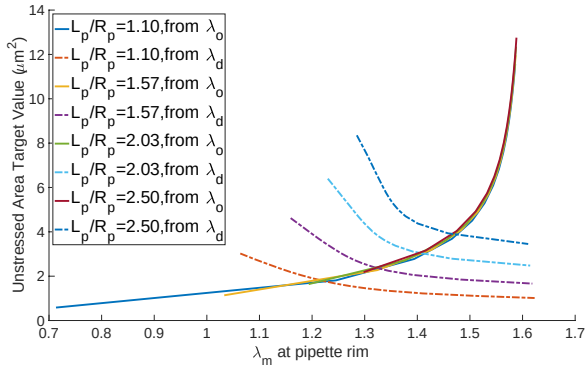

Figure S1. Intersecting curves show the solution points for four cases of increasing Lp/Rp. The four curves for the disk solutions overlap, and the four sets of solutions for the projections are labeled as shown.

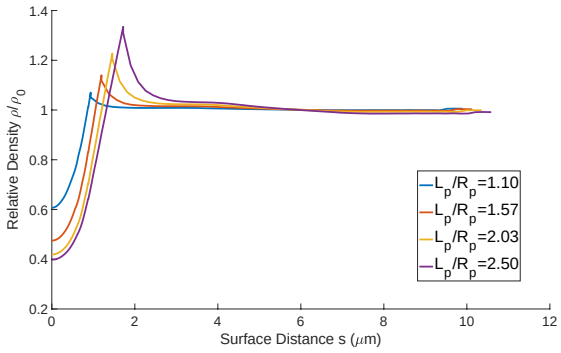

Figure S2. Distribution of density relative to the resting density ρ_0 over the surface of the cell. The distance s is measured along the surface from the tip of the projection.

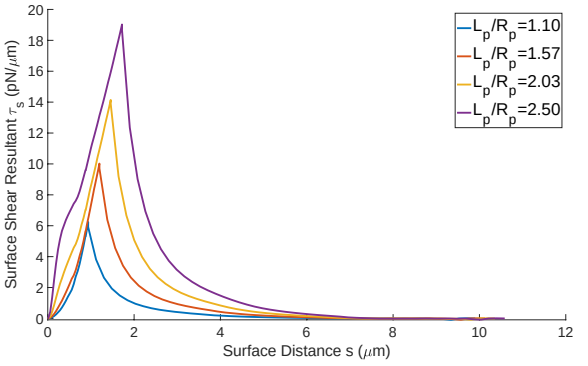

Figure S3. Distribution of the shear force resultant τ_s over the surface of the cell. The distance s is measured along the surface from the tip of the projection.

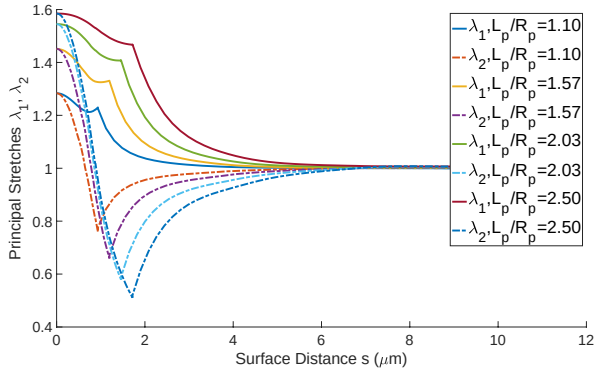

Figure S4. Distribution of the principal stretches over the surface of the cell. The distance s is measured along the surface from the tip of the projection.

APPENDIX B. Detailed derivations of the constitutive models

Derivation of the simplified constitutive model

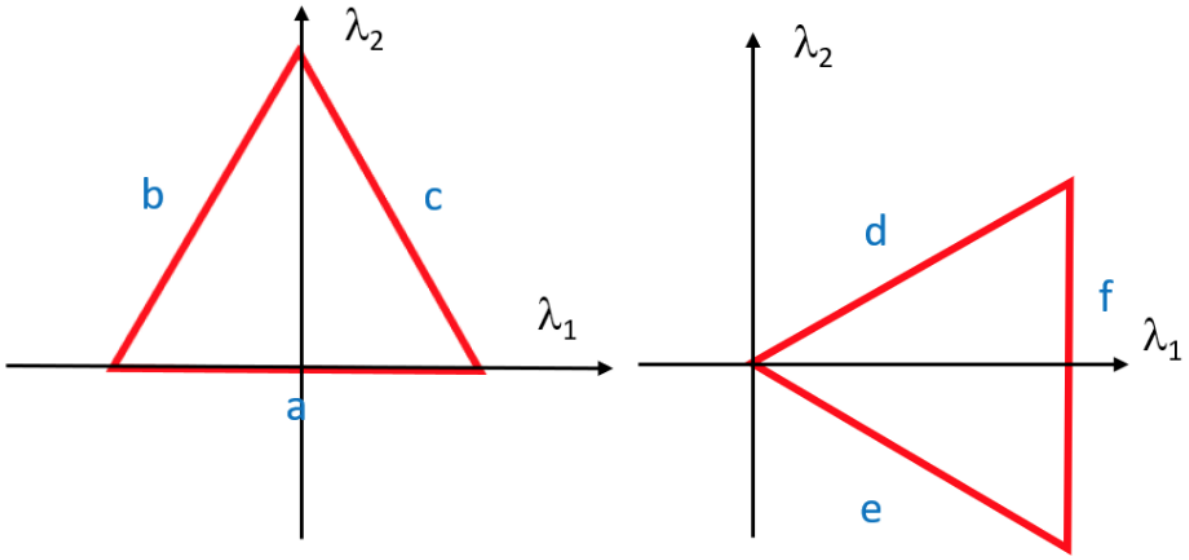

Figure S5. Network elements having six different molecular orientations in the resting state. Directions of the principle stretch directions are as shown. Letters of the segments correspond to those in the energy expression (Eq. S8).

For a unit cell with two orientations shown in Figure S5, i.e. n = 6, the free energy density is:

$$\begin{aligned} w &= \frac{1}{4A_0}V_{WLC}(a) + 2V_{WLC}(b) + V_{WLC}(f) + 2V_{WLC}(d) + \frac{C}{4A} \\ &= \frac{2c_\beta}{3x_0^2}\left[\frac{3\lambda_1^2x_0^2 - 2\lambda_1^3x_0^3}{2-2\lambda_1x_0} + \frac{3(\lambda_1^2+3\lambda_2^2)x_0^2 - (\lambda_1^2+3\lambda_2^2)^{3/2}x_0^3}{1-\sqrt{\frac{\lambda_1^2}{4}-\frac{3\lambda_2^2}{4}}x_0}\right. \\ &\left. + \frac{3\lambda_2^2x_0^2 - 2\lambda_2^3x_0^3}{2-2\lambda_2x_0} + \frac{3(\lambda_2^2+3\lambda_1^2)x_0^2 - (\lambda_2^2+3\lambda_1^2)^{3/2}x_0^3}{1-\sqrt{\frac{\lambda_2^2}{4}-\frac{3\lambda_1^2}{4}}x_0}\right] + \frac{C}{4A} \end{aligned} \tag{S8}$$

where $c_\beta = \frac{k_BT\rho_0s_0}{8p\lambda_{max}} = \frac{\sqrt{3}k_BT}{4ps_{max}}$, and the principal stress resultants are given by Eq. 5 and Eq. 6 as

$$\tau_1^{sk} = \frac{4c_\beta}{3}\frac{\lambda_1}{\lambda_2}\left[\frac{\frac{1}{4(1-\lambda_1 x_0)^2} + \lambda_1 x_0 - \frac{1}{4}}{\lambda_1 x_0} + \frac{\frac{1}{4\left(1-\sqrt{\frac{\lambda_1^2}{4}+\frac{3\lambda_2^2}{4}}x_0\right)^2} + \lambda_1 x_0 - \frac{1}{4}}{\sqrt{\frac{\lambda_1^2}{4}+\frac{3\lambda_2^2}{4}}x_0}\frac{1}{2}\right.$$
$$\left. + \frac{\frac{1}{4\left(1-\sqrt{\frac{\lambda_2^2}{4}+\frac{3\lambda_1^2}{4}}x_0\right)^2} + \lambda_1 x_0 - \frac{1}{4}}{\sqrt{\frac{\lambda_2^2}{4}+\frac{3\lambda_1^2}{4}}x_0}\frac{3}{2}\right] - \frac{c_\beta c_\alpha}{\lambda_1^2\lambda_2^2} \quad (S9)$$

$$\tau_2^{sk} = \frac{4c_\beta}{3}\frac{\lambda_2}{\lambda_1}\left[\frac{\frac{1}{4(1-\lambda_2 x_0)^2} + \lambda_2 x_0 - \frac{1}{4}}{\lambda_2 x_0} + \frac{\frac{1}{4\left(1-\sqrt{\frac{\lambda_2^2}{4}+\frac{3\lambda_1^2}{4}}x_0\right)^2} + \lambda_1 x_0 - \frac{1}{4}}{\sqrt{\frac{\lambda_1^2}{4}+\frac{3\lambda_2^2}{4}}x_0}\frac{1}{2}\right.$$
$$\left. + \frac{\frac{1}{4\left(1-\sqrt{\frac{\lambda_2^2}{4}+\frac{3\lambda_1^2}{4}}x_0\right)^2} + \lambda_1 x_0 - \frac{1}{4}}{\sqrt{\frac{\lambda_1^2}{4}+\frac{3\lambda_2^2}{4}}x_0}\frac{3}{2}\right] - \frac{c_\beta c_\alpha}{\lambda_1^2\lambda_2^2} \quad (S10)$$

The shear stress, mean stress, shear modulus, and area modulus are given as

$$\tau_s^{sk} = \frac{\tau_1^{sk} - \tau_2^{sk}}{2} = \frac{1}{2}\left(\frac{\partial w}{\partial \lambda_1}\frac{1}{\lambda_2} - \frac{\partial w}{\partial \lambda_2}\frac{1}{\lambda_1}\right) \quad (S11)$$

$$\tau_a^{sk} = \frac{\tau_1^{sk} + \tau_2^{sk}}{2} = \frac{1}{2}\left(\frac{\partial w}{\partial \lambda_1}\frac{1}{\lambda_2} + \frac{\partial w}{\partial \lambda_2}\frac{1}{\lambda_1}\right) \quad (S12)$$

$$\mu = \left|\frac{2\tau_s^{sk}\lambda_1^2\lambda_2^2}{\lambda_1^2 - \lambda_2^2}\right| \quad (S13)$$

$$K = \frac{\partial \tau_a}{\partial \alpha} = \frac{\partial^2 w}{\partial \alpha^2} \quad (S14)$$

$$\tau_s^{sk} = \frac{2c_\beta}{3\lambda_1\lambda_2}\left[\frac{\frac{1}{4(1-\lambda_1 x_0)^2}+\lambda_1 x_0-\frac{1}{4}}{\lambda_1 x_0}\lambda_1^2 - \frac{\frac{1}{4(1-\lambda_2 x_0)^2}+\lambda_2 x_0-\frac{1}{4}}{\lambda_2 x_0}\lambda_2^2\right.$$
$$+\frac{\frac{1}{4\left(1-\sqrt{\frac{\lambda_1^2}{4}+\frac{3\lambda_2^2}{4}}x_0\right)^2}+\lambda_1 x_0-\frac{1}{4}}{\sqrt{\frac{\lambda_1^2}{4}+\frac{3\lambda_2^2}{4}}x_0}\left(\frac{\lambda_1^2}{2}-\frac{3\lambda_2^2}{2}\right)+\frac{\frac{1}{4\left(1-\sqrt{\frac{\lambda_2^2}{4}+\frac{3\lambda_1^2}{4}}x_0\right)^2}+\lambda_1 x_0-\frac{1}{4}}{\sqrt{\frac{\lambda_2^2}{4}+\frac{3\lambda_1^2}{4}}x_0}\left(\frac{3\lambda_1^2}{2}-\frac{\lambda_2^2}{2}\right) \quad \text{(S15)}$$

$$\tau_a^{sk} = \frac{2c_\beta}{3\lambda_1\lambda_2}\left[\frac{\frac{1}{4(1-\lambda_1 x_0)^2}+\lambda_1 x_0-\frac{1}{4}}{\lambda_1 x_0}\lambda_1^2 + \frac{\frac{1}{4(1-\lambda_2 x_0)^2}+\lambda_2 x_0-\frac{1}{4}}{\lambda_2 x_0}\lambda_2^2\right.$$
$$+\frac{\frac{1}{4\left(1-\sqrt{\frac{\lambda_1^2}{4}+\frac{3\lambda_2^2}{4}}x_0\right)^2}+\lambda_1 x_0-\frac{1}{4}}{\sqrt{\frac{\lambda_1^2}{4}+\frac{3\lambda_2^2}{4}}x_0}\left(\frac{\lambda_1^2}{2}+\frac{3\lambda_2^2}{2}\right)$$
$$\left.+\frac{\frac{1}{4\left(1-\sqrt{\frac{\lambda_2^2}{4}+\frac{3\lambda_1^2}{4}}x_0\right)^2}+\lambda_1 x_0-\frac{1}{4}}{\sqrt{\frac{\lambda_2^2}{4}+\frac{3\lambda_1^2}{4}}x_0}\left(\frac{3\lambda_1^2}{2}+\frac{\lambda_2^2}{2}\right)\right] - \frac{c_\beta c_\alpha}{(\lambda_1\lambda_2)^2} \quad \text{(S16)}$$

To simplify the stress expressions, we explore the fact that Eq. 3 is an interpolation formula to the original worm-like chain model. In other words, Eq. 3 gives exact results for low and high force limits, but only gives an approximate result in intermediate force range (15% relative error). To obtain a simplified strain energy function, we will make it exact for low and high force limits, but construct an interpolation formula of stress in terms of stretches rather than the force in terms of chain length *s* in Eq. 3.

Simplified constitutive model with area change

To simplify the expression of the shear stress resultant in Eq. S15, assume it can be approximated as the following interpolated forms

$$\tau_{ss}^{sk} = \frac{2c_\beta}{3x_0}[d_0 + d_1(\lambda_s - 1) + \frac{d_\infty \lambda_s}{(1 - \lambda_s\lambda_a x_0)^2}] \quad (S17)$$

where the deformation is expressed in terms of isotropic (λ_a) and shear (λ_s) coefficients $\lambda_a = \sqrt{\lambda_1\lambda_2} = \sqrt{\alpha + 1}$, $\lambda_s = \sqrt{\lambda_1/\lambda_2}$.

To determine the three coefficients (d_0, d_1, d_∞) we match the slope of Eq. 18 with Eq. 10 with n = 6 for the low force limit and the high force limit.

At the high force limit, $\lambda_s\lambda_a x_0 \sim 1$, where the protein chain is close to its contour length, with asymptotic expansion at the high force limit or Laurent expansion, we get:

$$\tau_s^{sk} \sim \frac{2c_\beta}{3x_0\lambda_a^2}\left[\frac{\lambda_a\lambda_s}{4(1 - \lambda_s\lambda_a x_0)^2} + O(1)\right] \quad (S18)$$

At the same time the simplified shear stress near the high force limit:

$$\tau_{ss}^{sk} \sim \frac{2c_\beta}{3x_0}\left[\frac{d_\infty \lambda_s}{(1 - \lambda_s\lambda_a x_0)^2} + O(1)\right]$$

By matching them we can get

$$d_\infty = \frac{1}{4\lambda_a} \quad (S19)$$

Enforcing $\tau_s^{sk} = 0\ for\ \lambda_s = 1$,which means no shear stress when there is no shear deformation, we found that:

$$\tau_{ss}^{sk} = \frac{2c_\beta}{3x_0}\left[d_0 + \frac{d_\infty}{(1 - \lambda_a x_0)^2}\right] = 0 \quad (S20)$$

so

$$d_0 = \frac{-1}{4\lambda_a x_0^2(\lambda_a - 1/x_0)^2}, \quad (S21)$$

We obtain d_1 by matching slopes in terms of λ_s near $\lambda_s = \lambda_a = 1$,which is equivalent to matching the initial shear modulus μ_0. At the low shear force point, where there is no shear

deformation,

$$\mu = \frac{2\tau_{ss}^{sk}\lambda_1^2\lambda_2^2}{\lambda_1^2-\lambda_2^2}\bigg|_{\lambda_s\to 1} = \frac{c_\beta}{3x_0}\left[\frac{1+\lambda_a x_0}{4\lambda_a(1-\lambda_a x_0)^3} + d_1(\lambda_a x_0)\right]$$

Assuming the shear modulus under area deformation is only a function of expanded chain length $\lambda_a x_0$,

$$\mu = \mu(\lambda_a x_0),$$

which indicates $\frac{c_\beta}{3x_0} d_1 = f(\lambda_a x_0)$ is also a function of $\lambda_a x_0$. This means that during area expansion, the shear modulus hardening is independent of s_0 and depends only on the expanded chain length $\lambda_a s_0$. Then we have

$$\mu_0 = c_\beta\left(c_\alpha + \frac{3x_0 - x_0^2}{4(1-x_0)^3}\right) = \frac{c_\beta}{3x_0}\left[\frac{1+x_0}{4(1-x_0)^3} + d_1(x_0)\right]$$

$$\frac{d_1(x_0)}{x_0} = \frac{48(x_0)^4 - 153(x_0)^3 + 171(x_0)^2 - 71(x_0) + 1}{4x_0(x_0-1)^3},$$

then:

$$\frac{d_1(\lambda_a x_0)}{x_0} = \frac{48(\lambda_a x_0)^4 - 153(\lambda_a x_0)^3 + 171(\lambda_a x_0)^2 - 71(\lambda_a x_0) + 1}{4\lambda_a x_0(\lambda_a x_0 - 1)^3} \qquad (S22)$$

So

$$d_1 = \frac{48(\lambda_a x_0)^4 - 153(\lambda_a x_0)^3 + 171(\lambda_a x_0)^2 - 71(\lambda_a x_0) + 1}{4\lambda_a(\lambda_a x_0 - 1)^3} \qquad (S23)$$

Although the above equations were derived from the case of *n* = 6, it works for arbitrary n > 2, assuming isotropy.

If the area is incompressible, our formulation is reduced to

$$\tau_s^{sk} = \frac{2c_\beta}{3x_0}\left[c_0 + c_1(\lambda_1 - 1) + \frac{\lambda_1}{4(1-\lambda_1 x_0)^2}\right] \qquad (S24)$$

where $c_0 = \frac{-1}{4(1-x_0)^2}$

$$c_1 = \frac{48{x_0}^4 - 153{x_0}^3 + 171{x_0}^2 - 71x_0 + 1}{4(x_0 - 1)^3}$$

$$\mu = \frac{2\tau_s^{sk}}{\lambda_1^2 - \lambda_2^2} = \frac{4c_\beta}{3x_0(\lambda_1^2 - \lambda_2^2)}\left[c_0 + c_1(\lambda_1 - 1) + \frac{\lambda_1}{4(1-\lambda_1 x_0)^2}\right] \quad (S25)$$

This equation also works for arbitrary n>2.

Finite thermoelasticity and stresses of 2D hyperelastic membranes

Let's consider the cytoskeletal network as a 2D hyperelastic material without any remodeling or dissipation. The Cauchy stress of a hyperelastic material is given as

$$\boldsymbol{\sigma} = \frac{2}{J}\boldsymbol{F}\frac{\partial w}{\partial \boldsymbol{C}}\boldsymbol{F}^T \quad (S26)$$

where $w = H\text{-}TS = w(\boldsymbol{F},T)$ is the free energy density (measured per unit volume), $\boldsymbol{C} = \boldsymbol{F}^{\boldsymbol{T}}\boldsymbol{F}$ is the right Cauchy-Green deformation tensor, **F** is the deformation gradient, and $J = det(\mathbf{F})$. H is the enthalpy (internal energy, per unit volume), T is the temperature, and S is the entropy (per unit volume). If the material is isotropic, invariants of the deformation can be used to simplify the stress expression, so that the Cauchy stress resultant of a 2D isotropic hyperelastic material in Eq. S26 is reduced to

$$\boldsymbol{\tau} = \boldsymbol{\sigma}h = \tau_a\boldsymbol{I} + \frac{\mu}{(\alpha+1)^2}\left(\boldsymbol{B} - \frac{\mathrm{trace}(\boldsymbol{B})}{2}\boldsymbol{I}\right) \quad (S27)$$

where

$$\tau_a = \frac{\partial \mathrm{w}}{\partial \alpha}, \mu = \frac{\partial \mathrm{w}}{\partial \beta}, \boldsymbol{B} = \boldsymbol{F}\boldsymbol{F}^{\boldsymbol{T}}, \boldsymbol{F} = \frac{\partial \mathbf{x}}{\partial \mathbf{X}}$$

where τ_α and μ are defined as the mean stress resultant and shear modulus and $\boldsymbol{B}$ is the left Cauchy-Green deformation tensor. The area invariant, $\alpha = \lambda_1\lambda_2 - 1$, and the shear invariant $\beta = (\lambda_1/\lambda_2 +$

λ_2/λ_1 - 2)/2 are those defined by Evans and Skalak (1), where λ_1 and λ_2 are the principal stretch ratios and h is the thickness. $\mathbf{x}$ is the current coordinate vector and $\mathbf{X}$ is the initial coordinate vector.

The principal stress resultants in the skeleton are related to the energy by:

$$\tau_1^{sk} = \frac{1}{\lambda_2}\frac{dw}{d\lambda_1} \tag{S28}$$

$$\tau_2^{sk} = \frac{1}{\lambda_1}\frac{dw}{d\lambda_2} \tag{S29}$$

To convert from the discrete form of the potential (expressed in terms of individual molecules) to a continuous form, the different deformation experienced by molecules having different orientations relative to the principal axes of deformation must be considered. We apply the affine assumption, namely, that the endpoints of the molecule follow the corresponding points in the continuum deformation. With this affine deformation assumption, we do not need to be concerned about the detailed connectivity between molecules. Taking s_o as the resting molecular length, the molecular extension (s/s_o) is related to the material extension ratios by

$$s^2 = \lambda_1^2 x_{0,i}^2 + \lambda_2^2 y_{0,i}^2$$

$$\left(\frac{s}{s_0}\right)_i^2 = \lambda_1^2\, cos^2\,\theta_{0,i} + \lambda_2^2\, sin^2\,\theta_{0,i} \tag{S30}$$

where $\theta_{0,i} = \frac{i\pi}{n}, i \in (1, n)$ is the angle between the molecular vector for orientation i and the principal axis of extension in the resting state. The energy per unit area must be summed over molecular orientations.

From Eq. 1 and. Eq. 2 we obtain

$$w_{total} = \sum_{i=1}^{n} V_{eff}(s)/A = \sum_{i=1}^{n} \frac{k_B T s_{max}}{4pA}\left(\frac{s}{s_{max}}\right)^2 \cdot \frac{3-2s/s_{max}}{1-s/s_{max}} cos^2\,\theta_{0,i}$$

Substituting this into Eq. S28 and Eq. S29 we arrive at

$$\tau_1^{sk} = \frac{1}{\lambda_2}\frac{dw}{d\lambda_1} = \frac{1}{\lambda_2}\frac{\partial w}{\partial s}\frac{\partial s}{\partial \lambda_1} = \frac{\lambda_1}{\lambda_2}\frac{\partial w}{\partial s}\frac{{s_0}^2}{s}cos^2\,\theta_{0,i}$$

$$= \sum_{i=1}^{n} \frac{k_B T}{4(p/s_0)A}\frac{\lambda_1}{\lambda_2}\left[\frac{1}{4(1-s/s_{max})^2} - \frac{1}{4} + s/s_{max}\right]\frac{s}{s_o}cos^2\,\theta_{0,i}$$

$$= \sum_{i=1}^{n} \frac{k_B T}{4(p/s_0)A\lambda_{max}}\frac{\lambda_1}{\lambda_2}\frac{6\lambda_{max}^2 - 9\lambda_{max}(s/s_o)_i + 4(s/s_o)_i^2}{(\lambda_{max} - (s/s_o)_i)^2}cos^2\,\theta_{0,i}$$

Since $\rho_0 = \frac{n}{A}$ in this case,

$$\tau_1^{sk} = c_\beta\left[\frac{2}{n}\frac{\lambda_1}{\lambda_2}\sum_{i=1}^{n}\left(cos^2\,\theta_{o,i}\cdot P_i\left(\frac{s}{s_o}\right)\right) - \frac{c_\alpha}{{\lambda_1}^2{\lambda_2}^2}\right] \quad \text{(S31)}$$

$$\tau_2^{sk} = c_\beta\left[\frac{2}{n}\frac{\lambda_2}{\lambda_1}\sum_{i=1}^{n}\left(sin^2\,\theta_{o,i}\cdot P_i\left(\frac{s}{s_o}\right)\right) - \frac{c_\alpha}{{\lambda_1}^2{\lambda_2}^2}\right] \quad \text{(S32)}$$

where

$$c_\alpha = \frac{6\lambda_{max}^2 - 9\lambda_{max} + 4}{(\lambda_{max} - 1)^2}$$

$$c_\beta = \frac{k_B T \rho_0}{8(p/s_0)\lambda_{max}}$$

and,

$$P_i(s/s_o) = \frac{6\lambda_{max}^2 - 9\lambda_{max}(s/s_o)_i + 4(s/s_o)_i^2}{(\lambda_{max} - (s/s_o)_i)^2}$$

Derivation of the area modulus K

For this 2D isotropic hyperelastic material, we can calculate the area modulus as:

$$K^{sk} \equiv \left(\frac{\partial \tau_\alpha^{sk}}{\partial \alpha}\right)_\beta \quad (S33)$$

with the stress expression

$$\tau_1^{sk} = c_\beta\left[\frac{2}{n}\frac{\lambda_1}{\lambda_2}\sum_{i=1}^{n}\left(cos^2\,\theta_{o,i}\cdot P_i\left(\frac{s}{s_o}\right)\right) - \frac{c_\alpha}{{\lambda_1}^2{\lambda_2}^2}\right],$$

$$\tau_2^{sk} = c_\beta \left[\frac{2}{n} \frac{\lambda_2}{\lambda_1} \sum_{i=1}^{n} \left(sin^2\,\theta_{o,i} \cdot P_i\left(\frac{s}{s_o}\right) \right) - \frac{c_\alpha}{{\lambda_1}^2 {\lambda_2}^2} \right],$$

the tension can be calculated and simplified:

$$\tau_\alpha^{sk} = \frac{\tau_1^{sk} + \tau_2^{sk}}{2} = c_\beta \left[\frac{1}{n} \sum_{i=1}^{n} \left(\frac{\lambda_1}{\lambda_2} cos^2\,\theta_{o,i} \cdot P_i\left(\frac{s}{s_o}\right) + \frac{\lambda_2}{\lambda_1} sin^2\,\theta_{o,i} \cdot P_i\left(\frac{s}{s_o}\right) \right) - \frac{c_\alpha}{{\lambda_1}^2 {\lambda_2}^2} \right]$$

$$= c_\beta \left[\frac{1}{n\lambda_1\lambda_2} \sum_{i=1}^{n} \left(\lambda_1^2\, cos^2\,\theta_{0,i} + \lambda_2^2\, sin^2\,\theta_{0,i}\right) P_i\left(\frac{s}{s_o}\right) - \frac{c_\alpha}{{\lambda_1}^2 {\lambda_2}^2} \right]$$

$$= c_\beta \left[\frac{1}{n\lambda_1\lambda_2} \sum_{i=1}^{n} x^2 P_i(x) - \frac{c_\alpha}{{\lambda_1}^2 {\lambda_2}^2} \right] = c_\beta \left[\frac{1}{n(1+\alpha)} \sum_{i=1}^{n} x^2 P_i(x) - \frac{c_\alpha}{(1+\alpha)^2} \right] \qquad (B34)$$

where $x_i^2 = \left(\frac{s}{s_0}\right)_i^2 = \lambda_1^2\, cos^2\,\theta_{0,i} + \lambda_2^2\, sin^2\,\theta_{0,i}$. From the expression of α and β in terms of λ_1 and λ_2, we can know:

$$\frac{\partial \lambda_1}{\partial \alpha} = \frac{1}{2\lambda_2}, \frac{\partial \lambda_2}{\partial \alpha} = \frac{1}{2\lambda_1} \qquad (S35)$$

then $\frac{\partial x_i}{\partial \alpha}$ can be gained from Eq. S30

$$2x_i \frac{\partial x_i}{\partial \alpha} = 2\lambda_1\, cos^2\,\theta_{0,i}\,/(2\lambda_2) + 2\lambda_2\, sin^2\,\theta_{0,i}\,/(2\lambda_1)$$

$$\frac{\partial x_i}{\partial \alpha} = \lambda_1\, cos^2\,\theta_{0,i}\,/\lambda_2 + \lambda_2\, sin^2\,\theta_{0,i}\,/\lambda_1 = \frac{x_i^2}{2x_i\lambda_1\lambda_2} = \frac{x_i}{2(1+\alpha)} \qquad (S36)$$

Also from Eq. 9, we have

$$\frac{\partial P_i(x)}{\partial x_i} = \frac{3\lambda_{max}^2 - \lambda_{max} x_i}{(\lambda_{max} - x_i)^3} \qquad (S37)$$

Everything can be expressed in terms of α, therefore,

$$K = \partial c_\beta \left[\frac{1}{n(1+\alpha)} \sum_{i=1}^{n} x_i^2 P_i(x) \; - \; \frac{c_\alpha}{(1+\alpha)^2} \right] / \partial(\alpha)$$

$$= c_\beta \left[\frac{-1}{n(1+\alpha)^2} \sum_{i=1}^{n} {x_i}^2 P_i(x_i) \; + \frac{2}{n(1+\alpha)} \sum_{i=1}^{n} \frac{\partial x_i}{\partial \alpha} x_i P_i(x_i) \; + \frac{1}{n(1+\alpha)} \sum_{i=1}^{n} \frac{\partial x_i}{\partial \alpha} \frac{\partial P_i}{\partial x_i} {x_i}^2 \right.$$

$$\left. + \; \frac{2c_\alpha}{(1+\alpha)^3} \right]$$

$$= c_\beta \left[\frac{-1}{n(1+\alpha)^2} \sum_{i=1}^{n} {x_i}^2 P_i(x) \; + \frac{1}{n(1+\alpha)^2} \sum_{i=1}^{n} {x_i}^2 P_i(x) \; + \frac{1}{n(1+\alpha)} \sum_{i=1}^{n} \frac{\partial x_i}{\partial \alpha} \frac{\partial P_i}{\partial x_i} {x_i}^2 \; + \; \frac{2c_\alpha}{(1+\alpha)^3} \right] (S38)$$

So

$$K = c_\beta \left[\frac{1}{n(1+\alpha)} \sum_{i=1}^{n} \frac{x_i}{2(1+\alpha)} \frac{\partial P_i}{\partial x_i} {x_i}^2 + \; \frac{2c_\alpha}{(1+\alpha)^3} \right]$$

$$= \frac{c_\beta}{2n(1+\alpha)^2} \left[\sum_{i=1}^{n} {x_i}^3 \; \frac{3\lambda_{max}^2 - \lambda_{max} x}{(\lambda_{max} - x)^3} \right] + \; \frac{2c_\beta c_\alpha}{(1+\alpha)^3} \qquad (S39)$$

Two special cases of Eq. S39 are of interest. The first is the purely isotropic deformation (no shear). In this case $x = x_i = \lambda_1 = \lambda_2 = s_i/s_o = \lambda_{iso}$, and the expression reduces to:

$$K^{sk}|_{iso} = \frac{c_\beta}{2nx^4} \left[\sum_{i=1}^{n} x^3 \; \frac{3\lambda_{max}^2 - \lambda_{max} x}{(\lambda_{max} - x)^3} \right] + \; \frac{2c_\beta c_\alpha}{x^6} = \frac{c_\beta}{2x} \frac{3\lambda_{max}^2 - \lambda_{max} x}{(\lambda_{max} - x)^3} + \; \frac{2c_\beta c_\alpha}{x^6} \qquad (S40)$$

The second is the value for this coefficient in the resting state K_0^{sk}, i.e. in the limit as $x=\lambda_{iso} \rightarrow 1.0$:

$$K_0^{sk} = c_\beta \left(2c_\alpha + \frac{3\lambda_{max}^2 - \lambda_{max}}{2(\lambda_{max} - 1)^3} \right) \qquad (S41)$$

We can also derive an expression for the modulus μ for an isotopic deformation:

$$\mu_{iso} = c_\beta x^2 \left(\frac{6\lambda_{max}^2 - 9x\lambda_{max} + 4x^2}{(\lambda_{max} - x)^2} + \frac{x(3\lambda_{max}^2 - x\lambda_{max})}{4(\lambda_{max} - x)^3} \right) \quad (S42)$$

APPENDIX C. Analysis of micropipette aspiration with cytoskeletal area change

Here we consider the area change of the cytoskeleton when deriving the relationship between pressure and aspiration length in micropipette experiments. Assuming the area change of the cytoskeleton outside of the pipette is a uniform small constant α_0, the deformation can be obtained from the mass conservation and total area conservation as

$$\pi R_0^2 \rho_0 = \frac{\pi(r^2 - R_p^2)\rho_0}{1 + \alpha_0} + m_{inside} \quad (S43)$$

Since

$$\lambda_1 = \frac{(1 + \alpha_0)R_0}{r} \quad (S44)$$

then we have

$$\frac{dr}{d\lambda_1} = \frac{\lambda_1 r}{1 + \alpha_0 - \lambda_1^2} \quad (S45)$$

$$\tau_{1,tip}^{sk} = \int_{R_p}^{\infty} \frac{\left(\tau_1^{sk} - \tau_2^{sk}\right)dr}{r}$$

$$= \int_{\lambda_L}^{\sqrt{1+\alpha_0}} \frac{2\tau_s^{sk}}{r}\frac{dr}{d\lambda_1}d\lambda_1$$

$$= \int_{\lambda_L}^{\sqrt{1+\alpha_0}} \frac{4c_\beta}{3x_0}[d_0 + d_1(\lambda_s - 1) + \frac{d_\infty \lambda_s}{(1-\lambda_s\lambda_a x_0)^2}]\frac{\lambda_1}{1+\alpha_0-\lambda_1^2}d\lambda_1$$

$$= \int_{\lambda_L'}^{1} \frac{4c_\beta}{3x_0'}[d_0 + d_1(\lambda_s - 1) + \frac{d_\infty \lambda_s}{(1-\lambda_s\lambda_a x_0')^2}]\frac{\lambda_s}{1-\lambda_s^2}d\lambda_s$$

$$= \frac{4c_\beta}{3x_0'}\left[D_0' + D_1'\lambda_L' + D_2'\ln\left(\frac{\lambda_L'+1}{2}\right) + D_3'\ln\left(\frac{1-x_0'}{1-x_0'\lambda_L'}\right) + \frac{D_4'}{1-x_0'\lambda_L'}\right] \quad (S46)$$

Thus

$$R_p\Delta P = \frac{8c_\beta}{3x_0^{'}}\left[D_0^{'} + D_1^{'}\lambda_L^{'} + D_2^{'}\ln\left(\frac{\lambda_L^{'}+1}{2}\right) + D_3^{'}\ln\left(\frac{1-x_0^{'}}{1-x_0^{'}\lambda_L^{'}}\right) + \frac{D_4^{'}}{1-x_0^{'}\lambda_L^{'}}\right] + 2T_\infty \quad (S47)$$

where $\lambda_L^{'} = \lambda_L/\sqrt{\alpha_0+1}$ is the stretch at the entrance of pipette, and

$$D_0' = \frac{-1}{4(1+x_0')^2(1-x_0')^2x_0'} - c_1'$$

$$D_1^{'} = c_1^{'} = \frac{48x_0^{'4} - 153x_0^{'3} + 171x_0^{'2} - 71x_0^{'} + 1}{4\left(x_0^{'}-1\right)^3}$$

$$D_2^{'} = -\frac{x_0^{'2}+1}{4(1+x_0^{'})^2(1-x_0^{'})^2} - c_1^{'}$$

$$D_3^{'} = \frac{x_0^{'}}{2\left(1+x_0^{'}\right)^2\left(1-x_0^{'}\right)^2}$$

$$D_4^{'} = \frac{1}{4(1-x_0^{'})^2}$$

$$x_0^{'} = x_0\sqrt{1+\alpha_0}$$

$$\lambda_L^{'} = \frac{\sqrt{\frac{A_{cell}\alpha_0}{\pi} + 2R_pL_p}}{R_p}$$

where α_0 is the average area change of the flat membrane and $A_{cell} = 135\mu m^2$ is the surface area of the RBC. $T_\infty = K_0\alpha_0$, and K_0 is the initial area modulus of the cytoskeleton. We choose $K_0 = 2\mu_0$, since α_0 is small.

λ_L' is a function of α_0

By assuming the total membrane area is constant (A_{cell} = 135 μm^2) due to the total area constraints from lipid bilayer and the membrane outside of the pipette has a uniform small constant α_0, we have

$$\text{Area conservation:} \quad A_{cell} = 2\pi L_p R_p + A_{out},$$
$$\text{Mass conservation:} \quad \rho_0 A_{cell} = m_{inside} + \frac{A_{out}\rho_0}{\alpha_0+1},$$
$$\text{Mass conservation:} \quad \rho_0 A_{cell} = \rho_0\pi\bar{R}_0^2 + \frac{A_{out}\rho_0}{\alpha_0+1},$$

A_{out} represents for the deformed membrane area outside of the pipette, m_{inside}/ρ_0 is the initial area of the membrane inside pipette.

By using A_{cell} = constant and eliminating A_{out}, we get

$$m_{inside} = \frac{A_{cell}\alpha_0 + 2\pi R_p L_p}{\alpha_0 + 1}\rho_0 \qquad (S48)$$

Since

$$\pi R_0^2\rho_0 = \frac{\pi(r^2 - R_p^2)\rho_0}{1+\alpha_0} + m_{inside} \qquad (S49)$$

then

$$\pi R_0^2 = \frac{\pi(r^2 - R_p^2) + A_{cell}\alpha_0 + 2\pi R_p L_p}{1+\alpha_0} \qquad (S50)$$

In particular, if $r = R_p$, we have

$$\bar{R}_0^2 = R_0^2|_{r=R_p} = \frac{m_{inside}}{\pi\rho_0} = \frac{\frac{A_{cell}\alpha_0}{\pi} + 2R_pL_p}{\alpha_0 + 1} \quad (S51)$$

Since

$$\lambda_1 = \frac{(1+\alpha_0)R_0}{r}$$

we can solve λ_L as

$$\lambda_L = \frac{(1+\alpha_0)R_0}{r}\bigg|_{r=R_p} = \frac{\sqrt{\alpha_0+1}\sqrt{\frac{A_{cell}\alpha_0}{\pi} + 2R_pL_p}}{R_p} \quad (S52)$$

$$\lambda_L' = \lambda_L/\sqrt{\alpha_0+1} = \frac{\sqrt{\frac{A_{cell}\alpha_0}{\pi} + 2R_pL_p}}{R_p} \quad (S53)$$

APPENDIX D. Cytoskeletal area change and effect of the number of orientations

Additional details on stress-strain behavior: Area change with stretch

One important difference between uniaxial extension ($\tau_2 = 0$) and pure shear (constant area) is that the area of the skeleton does change with extension, as would be expected for a compressible material. This is illustrated in Fig. S6, where a biphasic change in skeletal area is predicted, increasing for smaller extensions and decreasing as the extension approaches λ_{max}. For small extensions, the corresponding change in area does not depend strongly on the maximum stretch ratios (Fig. S6A), but unlike the stress resultants at large extensions, the changes in area expressed as a function of the extension normalized to λ_{max} do not collapse to a single curve, but rather reflect larger area expansions for larger values of λ_{max} over the entire range of values (Fig. S6B).

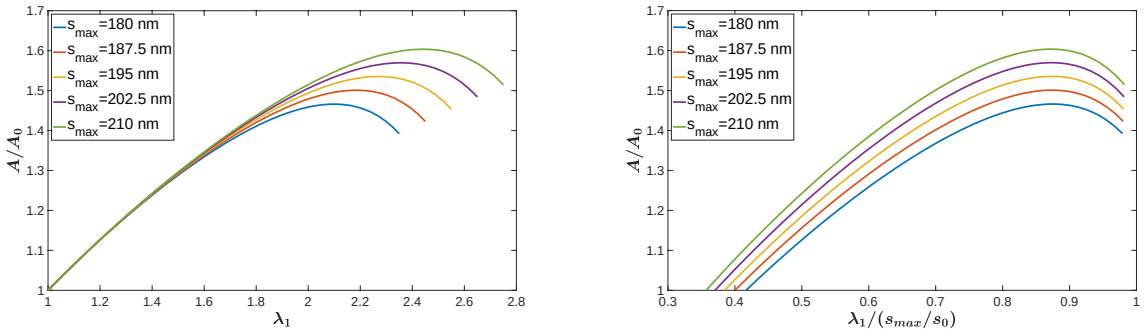

A. **B.**

Figure S6. A. The compressibility of the skeleton is reflected in increasing skeletal area with extension. Interestingly, the area increase reaches a maximum, and decreases at very high extensions. **B.** Unlike the stress resultant, the area change remains dissimilar for different values of λ_1/λ_{max} over the entire range of values. These curves reveal, however, that the maximum area increase occurs at approximately 86% of maximum extension for all λ_{max}.

Changes in shear modulus with area expansion

In Figure 2 of the manuscript we illustrate how the area modulus and the ratio of the area modulus change with membrane expansion. The shear modulus is also a function of both area

expansion and shear deformation. Both shear deformation (λ_1/λ_2) and skeletal dilation (α) cause molecules in the skeleton to approach their maximum length. Therefore, for larger ratios of λ_1/λ_2, the modulus approaches its asymptotic limit for smaller values of α. This is illustrated in Figure S7.

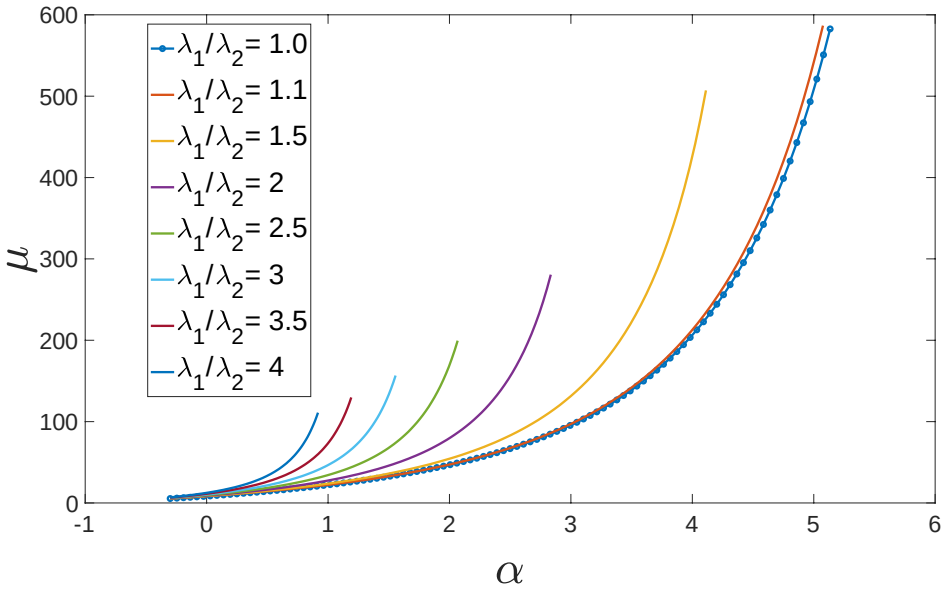

Figure S7. Dependence of the shear modulus on the area expansion for different ratios of stretches. The unit of the shear modulus is pN/ μm.

Increasing *n* to approximate a random network

Figure 2A in the main text shows how the calculated values of the stress resultant τ_1 vary with increasing n from 3 to 48. In this section we examine the dependence of the "error" introduced in calculating the stress resultant for different n, s_0 and s_{max}. For a given value of s_{max} the persistence length p is calculated according to the relationship given in the legend of Figure 7D:

$$p = c_1(6 - 9c_2/s_{max} + 4{c_2}^2/s_{max}^2)/(s_{max}/c_2 - 1)^2 \qquad (S54)$$

where c_1 = 0.0275 and c_2 = 101.85. We consider a simple uniaxial extension, both for the case of pure shear ($\lambda_2 = 1/\lambda_1$) and for the case $\tau_2 = 0$. As noted in the main text (Figure 2B), differences in calculated values of τ_1 for different n increase as the extension approaches $\lambda_{max} = s_0/s_{max}$. Therefore, we characterize the accuracy of the calculations in terms of the maximum extension of the material for which the difference in the calculated τ_1 is less than 1%. We find that this extension is within 0.5% of λ_{max} for all cases when comparing n = 48 with n = 96, indicating that n = 48 is a good approximation for $n \to \infty$. Therefore, the calculations were made for the maximum extension at which the calculated τ_1 is within 1% of the value calculated for n = 48.

We find that the maximum extensions for errors less than 1% depend on the specific value of s_0, but that the extensions expressed as a function of s_0/s_{max} fall on a single curve that is independent of s_{max} (Figure S8A). The maximum allowable extension increases with increasing n as expected (Figure S8B, Table S1). Similar results were obtained for pure shear deformations (Figures S8C and S8D). For modeling the skeleton with distributed values of s_0, we performed the weighted sum of contributions to τ_1 for the different values of s_0. The maximum allowable extensions for distributed values of s_0 are shown in Table S2. Note that when n is small (n = 3), significant errors can occur even for relatively modest extensions.

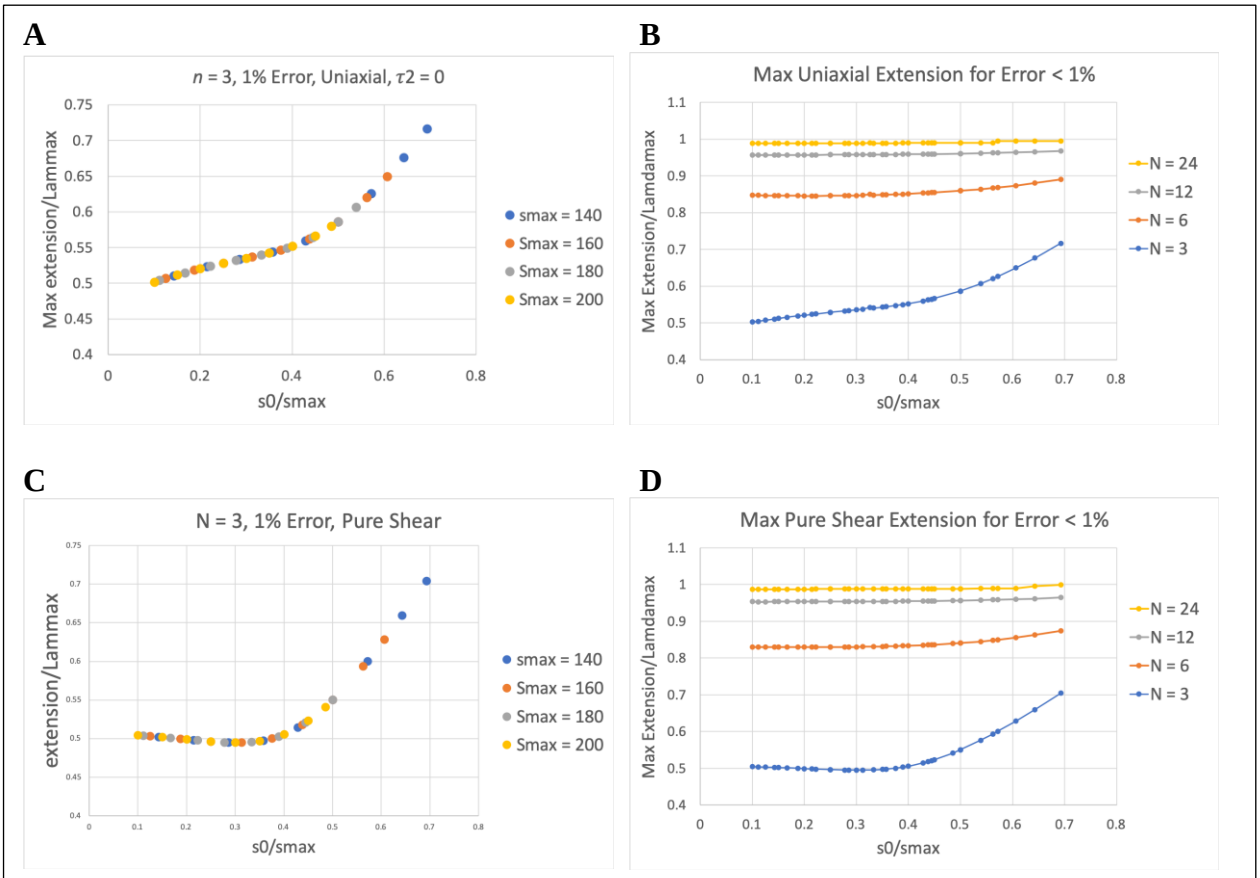

Figure S8. **A.** Maximum allowable extension for error < 1%, for uniaxial extension ($\tau_2 = 0$). When the extension and the values of s_0 are normalized by their maximum values, the curves are independent of s_{max}. **B.** The maximum allowable extension increases with increasing n. **C** and **D**. Similar results were obtained for pure shear deformation ($\lambda_2 = 1/\lambda_1$).

Table S1. Maximum allowable extension for 1% and 5% error (λ_1/λ_{max}, s_{max} = 180 nm)
Pure Shear

	1% error								
$n \setminus s_0$	20	30	40	50	60	70	80	90	97
3	0.5041	0.5012	0.4979	0.4953	0.4957	0.503	0.521	0.5502	0.5762
6	0.8298	0.8298	0.8298	0.8302	0.8312	0.833	0.8361	0.8407	0.8451
12	0.9532	0.9534	0.9534	0.9536	0.954	0.9545	0.9552	0.9564	0.9575
24	0.9874	0.9875	0.9876	0.9877	0.9878	0.988	0.9883	0.9886	0.9889
	5% error								
3	0.5785	0.5745	0.573	0.5686	0.5684	0.5685	0.5755	0.589	0.605
6	0.8677	0.8659	0.8686	0.8686	0.8668	0.8695	0.871	0.8744	0.8782
12	0.9656	0.9632	0.9649	0.9633	0.9654	0.9646	0.9671	0.9672	0.9671
24	0.9896	0.99	0.9905	0.9909	0.9914	0.9919	0.9924	0.9906	0.9911

Table S2. Maximum allowable extension (λ_1/λ_{max}, s_{max} = 180 nm), Uniaxial ($\tau_2 = 0$)

	1% error								
$n \setminus s_0$	20	30	40	50	60	70	80	90	97
3	0.5041	0.5149	0.5244	0.5323	0.54	0.5497	0.5645	0.5865	0.6065
6	0.8471	0.8458	0.8453	0.8459	0.8475	0.8503	0.8542	0.8594	0.8639
12	0.9569	0.9571	0.9571	0.9574	0.9579	0.9585	0.9593	0.9605	0.9614
24	0.9885	0.9886	0.9886	0.9888	0.9889	0.9891	0.9893	0.9896	0.9898
	5% error								
3	0.5963	0.5977	0.6046	0.6076	0.6132	0.6195	0.6277	0.6413	0.6522
6	0.8787	0.8799	0.8784	0.8813	0.882	0.884	0.8872	0.8896	0.8926
12	0.9662	0.9676	0.9692	0.9673	0.9692	0.9682	0.9704	0.9703	0.9700
24	0.9898	0.9902	0.9906	0.9911	0.9915	0.992	0.9925	0.993	0.9913

Table S3. Maximum allowable extension for distributed s_0 values, Pure Shear

s_{max}	200	180	160	140
λ_{max}	2.0619	1.8557	1.6495	1.4433
n	**Maximum allowable extension for error < 1%**			
3	1.31	1.20	1.11	1.05
6	1.84	1.66	1.48	1.31
12	1.99	1.79	1.59	1.40
24	2.04	1.84	1.63	1.43
	Maximum allowable extension for error < 5%			
3	1.47	1.33	1.20	1.09
6	1.89	1.71	1.52	1.34
12	2.00	1.81	1.61	1.41
24	2.04	1.84	1.64	1.43

Table S4. Maximum allowable extension for distributed s_0 values, Uniaxial ($\tau_2 = 0$)

s_{max} **(nm)**	200	180	160	140
λ_{max}	2.0619	1.8557	1.6495	1.4433
n	**Maximum allowable extension for error < 1%**			
3	1.41	1.29	1.18	1.09
6	1.86	1.68	1.50	1.33
12	1.99	1.80	1.60	1.41
24	2.04	1.84	1.64	1.43
	Maximum allowable extension for error < 5%			
3	1.56	1.42	1.28	1.15
6	1.91	1.72	1.53	1.35
12	2.01	1.81	1.61	1.41
24	2.05	1.84	1.64	1.43

Appendix E. Goodness of fit for different values of persistence length and maximum length.

Ideally one should be able to choose the best combination of molecular parameters (persistence length p and maximum molecular length s_{max}) based on the goodness of fit for the least squares regressions. Unfortunately, the resolution in the data is not sufficient to identify the best ordered pairs in the present case. The calculated sum of squared errors for each of the three different experiments presented in Figure 7 are tabulated below for the series of solution pairs for p and s_{max}. In two of the cases in Fig. 7, the lowest sum of squared errors occurs for small values of s_{max} and large values of p, but in the third case, the opposite is true. Which solution gives the lowest sum of squared errors depends critically on the data point at the highest pressure. Given this sensitivity, it would be inappropriate to infer too much about which of the possible combinations of s_{max} and p most accurately reflect true membrane properties.

Table S5 Fitting Error of Fig. 7A in the main text.

s_{max}	p	σ_{ap}	SSE	SSEp
130	48.5213	0.013069	0.99867	0.199734
135	37.12	1.07	1.122	0.2244
140	29.54	2.16	1.109	0.2218
145	24.19	3.38	0.911	0.1822
150	20.67	4.17	0.813	0.1626
160	15.54	6.28	0.674	0.1348
170	12.58	7.60	0.566	0.1132
180	10.61	8.74	0.498	0.0996
190	9.05	10.00	0.482	0.0964
200	8.03	10.64	0.4595	0.0919

R_p = 0.85 um. SSE: sum of the squared error. SSEp: sum of the squared error per data point.

Table S6 Fitting Error of Fig. 7B in the main text.

s_{max}	p	σ_{ap}	SSE	SSEp
130	52.3648	-3.4339	0.45421	0.090842
133	44.1032	-2.7385	0.37607	0.075214
135	39.8566	-2.3664	0.48052	0.096104
140	31.19	-0.89	0.5313	0.10626
145	26.26	-0.46	0.615	0.123
150	22.30	0.50	0.782	0.1564
160	16.71	2.56	1.083	0.2166
170	13.63	3.61	1.334	0.2668
180	11.39	4.80	1.54	0.308
190	9.82	5.77	1.948	0.3896
200	8.71	6.36	2.235	0.447

R_p = 0.55 um. SSE: sum of the squared error. SSEp: sum of the squared error per data point.

Table S7. Fitting Error of Fig. 7C in the main text.

s_{max}	p	σ_{ap}	SSE	SSEp
130	55.0781	-0.37773	3.5905	0.51292857
131	51.49	0	3.839	0.54842857
133	43.6	1.51	2.617	0.37385714
135	39.99	1.69	2.941	0.42014286
140	30.82	3.39	3.024	0.432
145	25.58	4.17	3.108	0.444
150	21.80	4.95	3.388	0.484
160	16.26	7.07	4.092	0.58457143
170	13.34	8.06	4.441	0.63442857
180	11.16	9.23	5.100	0.72857143
190	9.48	10.68	5.821	0.83157143
200	8.45	11.14	6.418	0.91685714

R_p = 0.55 um. SSE: sum of the squared error. SSEp: sum of the squared error per data point.

Supporting References.

1. Fung, Y. C., W. C. O. Tsang, and P. Patitucci. (1981). High-Resolution Data on the Geometry of Red-Blood-Cells. Biorheology 18(3-6):369-385.